DOI: 10.1111/cgf.12906
Eurographics Conference on Visualization (EuroVis) 2016
K.-L. Ma, G. Santucci, and J. van Wijk
(Guest Editors)

Volume 35 (2016), Number 3

Visual Analysis of Governing Topological Structures in Excitable Network Dynamics

Quynh Quang Ngo[1], Marc-Thorsten Hütt[2], and Lars Linsen[1]

[1]Department of Computer Science and Electrical Engineering, Jacobs University, Bremen, Germany
[2] Department of Life Sciences and Chemistry, Jacobs University, Bremen, Germany

Abstract

To understand how topology shapes the dynamics in excitable networks is one of the fundamental problems in network science when applied to computational systems biology and neuroscience. Recent advances in the field discovered the influential role of two macroscopic topological structures, namely hubs and modules. We propose a visual analytics approach that allows for a systematic exploration of the role of those macroscopic topological structures on the dynamics in excitable networks. Dynamical patterns are discovered using the dynamical features of excitation ratio and co-activation. Our approach is based on the interactive analysis of the correlation of topological and dynamical features using coordinated views. We designed suitable visual encodings for both the topological and the dynamical features. A degree map and an adjacency matrix visualization allow for the interaction with hubs and modules, respectively. A barycentric-coordinates layout and a multi-dimensional scaling approach allow for the analysis of excitation ratio and co-activation, respectively. We demonstrate how the interplay of the visual encodings allows us to quickly reconstruct recent findings in the field within an interactive analysis and even discovered new patterns. We apply our approach to network models of commonly investigated topologies as well as to the structural networks representing the connectomes of different species. We evaluate our approach with domain experts in terms of its intuitiveness, expressiveness, and usefulness.

Categories and Subject Descriptors (according to ACM CCS): I.3.8 [Computer Graphics]: Applications—

1 Introduction

One of the big questions in neuroscience is to discover the relation of functional and structural brain connectivity [Spo13]. In computational neuroscience and related fields of computational systems biology, structural connectivity is typically captured using networks, and computational models are employed to calculate the functional dynamics on these networks. The main question is then, which topological structures of the network govern the dynamical processes [GLHH12]. In computational biology, the main techniques are based on observing the correlation between structural and functional connectivity [MLHH08, MHKH15, GLHH12, Spo13]. However, even for rather simple networks, which and how topological structures govern the dynamics is not yet fully understood. For instance, in [MM13], the hierarchical modular brain connectivity is confirmed to be a stretch for criticality, i.e., the range of transition (or Griffiths) phases is stretched by the topology of the network. However, how the hierarchical modular connectivity results in the stretch still remains unclear [HH14]. The overarching goal of our work is to investigate what the network equivalents to classical spatio-temporal patterns [NM10] are and how topological structures such as hubs, modules, or hierarchies of modules relate to the processes behind spatio-temporal patterns of complex systems [MLHH08, MHKH15]. The objective of this paper is to propose an visual analysis approach to shed light on how topology and dynamics are related in dynamical processes on networks.

Our approach is based on an interactive analysis process using multiple coordinated views. The individual views visually encode relevant topological features of the network or relevant dynamical features of the processes. The interplay of the coordinated views allows for relating topology to dynamics. While purely analytical approaches typically focus on individual aspects based on some hypothesis that is being tested, using our approach, the analysis task can be addressed in a structured top-down approach. The individual contributions of our paper can be summarized as:

- Design of novel, suitable visual encodings for topological and dynamical features in excitable network dynamics.
- Interactive analysis approach for correlating topology to dynamics in excitable network dynamics.
- Reproduction of recent findings for topology-dynamics relations in excitable network dynamics.
- Detection of new items for topology-dynamics relations in excitable network dynamics.
- Application to the analysis of functional dynamics on structural networks representing the connectome of different species.

2 Background and Related Work

2.1 Network Topology

Networks represent local relationships between entities establishing a global connectivity. A network can be represented as a graph $G = (V, E)$ consisting of a set of vertices (or nodes) $V = \{v_1, v_2, \ldots, v_n\}$, which represent the entities, and a set of edges $E : V \times V$, which represent the pairwise relationships between nodes. These pairwise relationships between nodes can be stored in the form of an adjacency matrix A_G, a $|V| \times |V|$ matrix with binary entries. The graph provides the topology of the network.

2.1.1 Topological features

Our focus in terms of to-be-investigated topological structures lies on hubs, modules, or hierarchical modular structures, which have been reported to play a significant role for information propagation in excitable networks [MLHH08, GLHH12, HKH14]. A hub is defined as a node with a large number of edges to other nodes of the network, i.e., hubs are nodes with a high degree (number of incident edges). A module is described as a highly inter-connected subset of nodes, i.e., nodes within the module have many edges among them but only few to nodes outside the module. A hierarchy of modules refers to a modular structure, where within the modules there may be even more densely-connected subsets that form modules within the modules, which can be nested to form a hierarchy.

2.1.2 Network Models

Network models reflect specified global connectivity properties.

Scale-free Networks. A scale-free network is a network, whose degree distribution asymptotically follows a power law [BB03]. More precisely, the number of nodes with degree k is proportional to k^{-e}, where typically $e \in (2,3)$. Due to the tail-distribution degree, scale-free networks include some hubs as macroscopic structures. Many networks are conjectured to be scale-free including biological ones such as protein-protein interaction networks or others like the Internet or social networks [BB03]. Connectivity of neurons in the brain are also conjectured to be scale-free [EMB*09].

Hierarchical Modular Networks. A hierarchical modular network is a network that exhibits multiple levels of modular structures. Biological networks such as brain networks are reported to have hierarchical modular structures [MLB10, MLHH08]. We use a hierarchical modular network model [PS08] with two levels, where the network has three modules with five sub-modules each.

2.1.3 Empirical Networks

In addition to the computational network models described above, we also apply our methods to the analysis of empirical connectome networks. We used a cat brain network of 55 cortical and subcortical regions obtained by tract-tracing [SCKH04, HBO*00, HK04] and a macaque visual cortex network with 71 nodes [You93, RS10]. Both networks have modules and hubs as macroscopic structures.

2.1.4 Graph Drawing and Interactive Visual Analysis

The topology of networks is commonly visualized using adjacency matrix visualizations or node-link diagrams. Adjacency matrix visualizations show connectivity in the form of a matrix plot, which can reveal some information on the network's topology, if the correct order is established [Fek09, EDG*08]. Node-link diagrams are based on rendering the entities of the network as nodes and the relation between the entities as links (or edges). The main task to be solved is to position the nodes appropriately according to some design goal. Automatic layouts for node-link diagrams have been studied excessively in the graph drawing community [Tol96]. Different algorithms have been developed targeting graphs with certain properties. We refer to two recent of many existing surveys and books [GFV13, Tam13]. We also want to contrast our work against approaches for dynamic graph drawing [BBDW14, BPF14, Bra01], where graph topology changes over time. We, instead, want to visualize dynamical processes on graphs, where the dynamical processes are reflected by the changing properties of nodes over time, while the topological structure of the graph is static.

In the visualization community, approaches for network visualization enhance the visual encoding (e.g., the graph drawing) with interaction mechanisms that allow for an interactive visual analysis of the graphs [HMM00]. We again refer to a comprehensive recent survey on visual network analysis including visual encoding and interaction algorithms [vLKS*11]. Commonly, the graph analysis task is to investigate the relationships between entities in the graph and to assess the global graph structure [LPP*06, SSK14].

Such graph layout and interactive graph analysis approaches target the topology of the network and do not consider dynamical processes operating on the networks. We will be using visual encodings that reflect relevant topological structures and allow for an interactive analysis of their relation to the dynamical processes.

2.2 Network Dynamics

The dynamical processes can be represented by changes of (one or multiple) variables over time, where the variables are typically associated with the nodes of the network. Hence, using the graph notation, we can denote a dynamical process on a graph G by a dynamical function $g : V \times T \to \mathbb{R}^m$ that maps to each vertex $v_i \in V$ the value $g_{v_i}(t) \in \mathbb{R}^m$ at time $t \in T$ for a given time interval T. The state of the network which has n nodes at time $t \in T$ is then given by $< g_{v_1}(t), g_{v_2}(t), \ldots, g_{v_n}(t) >$. The current state of a network is updated by running a dynamical process (e.g., in the form of solving a differential equation) and considering the connectivity of the network. Hence, the topology impacts the dynamical process.

In network science, four prototypical dynamics have been identified, namely synchronization, information propagation, flow, and enabling/disabling [BLM*06]. We focus on the concept of information propagation through networks, i.e., how information is transported through the networks. Information propagation can be modeled using excitable dynamics.

2.2.1 Excitable Network Dynamics

The dynamical processes of excitable networks play an important role in biological modeling [MLHH08, MLMH06, HL09, MHKH15]. In particular, the excitation of neurons in the brain are modeled with such dynamics. At each time step, each node is in one of the three states: *susceptible* (S), *excited* (E), or *refractory*

(R). A well-known and widely used computational model for excitable dynamics is the forest-fire model, which updates the states over time as follows:

1. A node that is in the state *susceptible* enters the state *excited* in the subsequent time step, if at least one of its adjacent nodes is in the state *excited*. If there is no adjacent node that is *excited*, the *susceptible* node may still change to the state *excited* with a certain probability $f \in (0,1)$. This probability f is referred to as the spontaneous excitation rate.
2. A node that is in the state *excited* always becomes a *refractory* node in the subsequent time step.
3. A node that is in the state *refractory* enters the state *susceptible* in the subsequent step with a certain recovery probability $p \in (0,1)$.

Hence, for the forest-fire model, we have that $m = 1$ and the value range of the dynamical function g is categorical, although the three states appear in a certain cyclic order. The descriptions assume an undirected graph, i.e., a symmetric adjacency matrix. It can be applied to directed graphs by assuming that the excitation is only propagated between adjacent vertices, if the connecting edge goes from the *excited* to the *susceptible* node. The starting configuration assumes a uniformly random occurrence of the states *excited*, *susceptible* and *refractory*, i.e., the probability for each node to be in one of the three states is $\frac{1}{3}$.

2.2.2 Dynamical Features

Excitation Ratio. An intuitive pattern for hubs within excitable networks is that they are more likely to become excited more frequently. However, how this frequency is related to the degree of the hub may still be not obvious and worth investigating. We apply a simple local measure of activity of a node, which we call the excitation ratio. Let $g_{v_i}(t_j)$ be the state of node v_i at time step t_j. When considering a time series of length k, i.e., time steps $t_1,\ldots,t_k$, we count the occurrences of states susceptible (S), excited (E), and refractory (R) in the time series $< g_{v_i}(t_1),\ldots,g_{v_i}(t_k) >$, denoted by $\#S$, $\#E$, and $\#R$, respectively. Then, we can compute the ratio of a node being in the excited state E. Our interactive visual analysis revealed that the ratio $\frac{\#S}{\#S+\#R}$ is actually a more suitable descriptor, see Section 4.1. Intuitively, the count $\#E$ is implicitly represented here, as each node each time only remains in state E for one time step.

Co-activation. To investigate propagation patterns, we identified co-activation as a dynamical descriptor. The co-activation of two nodes is computed by comparing the time series of those nodes and counting how often the two nodes have a simultaneous activation (plus normalization). More precisely, assume nodes $v_i, v_j \in V$ and let $g_{v_i}(t_l)$ and $g_{v_j}(t_l)$ denote their state at time t_l for $l = 1,\ldots,k$, then the co-activation of the nodes v_i and v_j for a time series of length k is computed by

$$C_{ij}(k) = \frac{1}{k}\sum_{l=1}^{k} \delta((g_{v_i}(t_l) = E) \wedge (g_{v_j}(t_l) = E)),$$

where the δ-function is 1, if its Boolean argument is true, and 0 otherwise. The normalization assures that $C_{ij}(k) \in [0,1]$. The co-activation values for all pairs of nodes can be stored in an $n \times n$ co-activation matrix with $n = |V|$.

2.3 Relating Dynamics to Topology

2.3.1 Driving Questions

When analyzing the relation of dynamics to topology in excitable network dynamics, the following findings already have been made [HKH14]:

- Hubs lead to the propagation of waves of activity (or excitation).
- Modules lead to localized synchronization, which in turn results in a strong agreement between structural and functional connectivity.

Our first aim was to reproduce these findings within an interactive visual analysis tool, which shall help to add some intuition to the findings. Moreover, there are further aspects that the domain scientists (one of them being co-author of the paper) raised as interesting and relevant questions:

- Do the propagation of waves around hubs lead to interference in case of multiple hubs?
- Do the propagation waves around hubs depend on their degree and/or on the topological distance to the hubs (and to what extent)?
- Do hubs and modules communicate with each other in shaping co-activation patterns?

2.3.2 Analytical Approaches

Messe et al. [MHKH15] present correlations of structural and functional connectivity in excitable neural networks in the form of adjacency matrices. However, in case of hubs, adjacency matrices are of limited use, as they do not allow for an investigation of multiple layers around hubs. Müller-Linow et al. [MLHH08] present some results about co-activation waves around hubs using a purely analytical approach without any visual components. We were able to confirm those and to go beyond their findings. By observing the correlation pattern between structural and functional connectivity, Garcia et al. [GLHH12] found a negative correlation of hubs and modules in the cortical network of a cat brain. To do so, they destroyed hubs in the networks, which however changes the structure of the network and therefore weakens their argument. We address this question without altering the network topology. In general, purely analytical approaches assume that we have an idea about the governing topological structure to run the respective test.

2.3.3 Visual Approaches

Albrecht et al. [AKK*10] emphasize the lack of dedicated methods for visualizing dynamical process on networks. There have been some attempts to locally visualize dynamics at a node [JKS06], where time series are plotted at each node of the graph, but this does not allow for a global understanding of topological structures which trigger the dynamic processes. Similarly, approaches that use time as a third dimension over a 2D network layout to plot the time series [GAA04, FW10] make an analysis of the influence of topology on the dynamics hard, if not impossible. Ma et al. [MKF*15, MFL*16] visually analyzed memberships of nodes in dynamic modules of the functional network in brains. They investigated the relationship of the nodes' degree in the functional network with the spatial structure of the physical brain network.

Hence, they operate on a dynamically changing functional network, while the role of the static physical network's connectivity in shaping the dynamics was not analyzed. Toosi et al. [TPHL12] use a multidimensional scaling (MDS) approach to visualize dynamical processes on networks. They showed that animation can be used to show how topological clusters form by just looking into similarity of the nodes' time series. However, for the excitable networks example, they failed to identify the hub as a governing topological feature, which we address in this paper.

Recently, some visualization approaches investigated dynamics on networks in other application areas. Hadlak et al. [HSCW13] used a clustering of nodes based on temporal attributes to analyze wireless mesh networks. Steiger et al. [SBM*14] detected anomalies in sensor networks using a similarity plot of time-series data, which is related to the co-activation plot we propose as one of our three visual encodings. The MDS-based approach was reported to be reliable. However, the goals of these two approaches are fundamentally different from our goal, as we try to investigate, which topological structures of the networks are responsible for dynamical patterns.

3 Interactive Visual Analysis

3.1 Design Space and Choices

The target domain of our approach is to explore the relation between topology and dynamics. The topological connectivity structure is related to network and tree data, while the dynamics in the form of the nodes' time series data can be interpreted as a grid. The task is to analyze how network connectivity shapes dynamics. The relevant topological attributes comprise the degree of a node (of type ordinal), the distance of a node to a hubs (of type ordinal), and the membership of a node to a module (of type categorical). The relevant dynamical properties are based on the similarity or correlation of the nodes' time series.

To analyze how network connectivity shapes dynamics, the options are to embed both aspects (topology and dynamics) in one integrated view or to use separated views in a coordinated fashion. An integrated view can either be achieved by deploying a topological layout and embedding the time series data or by deploying a layout that reflects the dynamics and embedding the topological connectivity. The former approach fails to provide a global understanding of dynamical patterns and how topological structures trigger the dynamic processes (cf. [JKS06]), while in the latter approach topological properties get hidden when showing topological connectivity in a non-topological layout (cf. [TPHL12]). Thus, our interactive visual analysis approach is based on interacting with multiple coordinated views, each of which visually encodes a topological feature of the network or a dynamical feature of the dynamical process.

3.2 Visual Encoding of Topological Features

Degree Map. One goal of our analysis is to observe whether hubs are governing topological structures for the dynamical processes and how they interfere with each other and with other topological structures such as modules. Hence, we aimed at a visual encoding that allows us to easily detect hubs, rate the hubs' degree, and select and highlight hubs/nodes in a brushing-and-linking interaction concept. Using the size of the nodes as visual representation for encoding the degree of the nodes is an intuitive choice. Moreover, space-filling layouts allow for the optimal usage of the available screen space, which is desirable for selection and highlighting especially when using multiple coordinated views, i.e., when screen space is limited. Although we do not have a hierarchical structure of nodes, our design choice was to use a treemap approach, where the size of the rectangles is proportional to the degree of the corresponding node. We can apply the treemap generation approach to generate a suitable layout, if we assume that all nodes belong to the same level in the hierarchy. For best interpretability of size, we used the squarified treemap approach [BHVW00]. Nodes are first sorted by decreasing degree and then fed to the standard squarified treemap algorithm. For example, Figure 2(c) shows our *degree map* for the network in Figure 1. We can easily detect hubs and see how their degrees relate to the degrees of the other nodes. Also, nodes can easily be selected by mouse click and highlighted by color.

Other options for designing the degree map would have been using a linear structure such as bar charts or using other treemap layouts. Since we are operating with coordinated views, screen space is precious and space-filling layouts such as treemaps are preferable. Moreover, linear structures such as bar charts do not scale well with the number of items, leading to thin structures when trying to squeeze large data sets into the available screen space. Since we want to interact with the degree map, roundish objects are more suitable than longish ones such that squarified treemaps are favorable over other treemap layouts or bar charts (cf. [BHVW00]).

Adjacency Matrix. Adjacency matrices are known to clearly show modular structures, if a suitable order of the nodes is imposed. Hence, there was no need to introduce a new visual encoding for modules, especially since domain scientists are familiar with (static) adjacency matrix plots. For sorting the nodes, we used one of the state-of-the-art approaches, the barycenter order [Fek09, McG12]. Our adjacency matrix plots are not static though and we enhanced the display by adding a column to the right of the matrix that displays the current selection of nodes, see Figure 8(a). Since the matrix encodes pairs of nodes and our additional column encodes nodes only, we believe that this extension is a more suitable encoding of node selections.

3.3 Visual Encoding of Dynamical Features

Activity Plot. The activity plot shall encode how active individual nodes are, i.e., how often they are excited. As mentioned in Section 2.2.2, we count for each node the occurrences of states in the time series of length k and denote them by $\#S$, $\#E$, and $\#R$, respectively. We propose to use a barycentric-coordinates layout to depict the occurrences. Thus, we assign to a node with occurrences $\#S$, $\#E$, and $\#R$ the barycentric coordinates $(x_1,x_2,x_3) = (\frac{\#S}{k}, \frac{\#E}{k}, \frac{\#R}{k})$. Obviously, $x_1,x_2,x_3 \in [0,1]$ and $x_1+x_2+x_3 = 1$, i.e., all nodes are assigned a position within a triangle in a barycentric coordinate system, see Figure 2(a). The three corners of the triangle that span the barycentric space represent the three time series of a virtual node that is always in the state susceptible (depicted as a large green disk), a virtual node that is always in the state excitable (depicted as

a large red disk), and a virtual node that is always in the state refractory (depicted as a large black disk). More precisely, we consider three virtual nodes with time series $< S,\ldots,S >$, $< E,\ldots,E >$, and $< R,\ldots,R >$ and assign to them the barycentric coordinates $(1,0,0)$, $(0,1,0)$, and $(0,0,1)$, respectively.

Co-activation Plot. Since for the formation of patterns it is of importance to calculate how similar the dynamics of nodes are, we compute the co-activation matrix as described in Section 2.2.2. We propose to use a multi-dimensional scaling (MDS) technique [CC00] for the visual encoding of co-activation. The input to an MDS approach is a dissimilarity matrix $M = (M_{ij})$. We compute the entries of the matrix by $M_{ij} = 1 - C_{ij}$ for all i, j, where C denotes the co-activation matrix. Therefore, if the MDS projection exhibits a set of time series forming a cluster, then the corresponding nodes are supposed to be more often simultaneously excited than nodes whose time series were projected to a location outside the cluster.

To illustrate how the co-activation plot is interpreted, we generated the co-activation plot to a simple graph with tree topology, where the root represents a hub. For such a topology, it is to be expected that the hub, i.e., the root, functions as the main governing structure of the dynamical process. Figure 5(a) shows a node-link diagram of the tree in a radial layout with the nodes' color encoding the distance to the hub located at the center of the radial layout. The co-activation plot (b) exhibits some obvious clusters. Mapping the colors from the radial topological layout to the co-activation plot exhibits that each cluster consists of nodes of equal distance to the hub. Hence, nodes of same topological distance to the hub have higher co-activation than nodes of different topological distance. Hence, we can easily and intuitively observe the expected result for this simple example.

3.4 User Interaction

The main user interaction is based on switching between the two topological feature visualizations and the two dynamical feature visualizations and brushing and linking between them. Brushing and linking is based on selecting in one view and highlighting in the other view (cf. accompanying video). In addition, apart from the standard zooming and panning operations, we also support interactive filtering and updating the visual encoding based on the filtering operation.

Figures 2(a) and (b) show zooming and panning on a view and (b) and (c) show the brushing-and-linking idea by selecting a region of interest in the dynamics visualization (activity plot) and highlighting the selection using color in the topology visualization (degree map). Figures 6(a) and (b) show brushing and linking in the opposite direction, i.e., selecting in the topology visualization (degree map) and highlighting in the dynamics visualization (co-activation plot). Here, the highlighting is performed based on a color mapping of the topological distance of all nodes to the selected node. The color map used is a heat map, which has been shown to be suitable for ordinal data [War12], as the colors are ordered to have decreasing luminance for increasing topological distance. In the case of directed graphs, it may happen that there is no connected path between two nodes, i.e., the distance between them is ∞, which is encoded using black. Figures 8(a) and (b) show coordinated interactions with the adjacency matrix (topology) and the co-activation plot (dynamics). Here, the user selected regions of interest brushing the column next to the adjacency matrix. The user makes multiple selections and marks them using different colors. The respective selections are highlighted with the same color in the co-activation plot.

Figures 7(a)-(c) and Figures 8(b) and (d) show the filtering and updating on the co-activation plot. First, a filter is defined interactively by brushing a region of interest. Then, the visual encoding is updated by re-computing the co-activation plot for the chosen nodes only, i.e., other nodes are discarded when the MDS is recalculated.

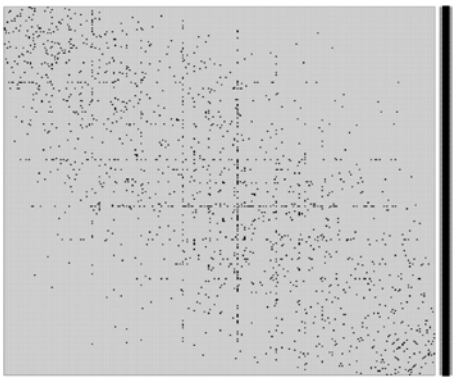

Figure 1: *Adjacency matrix of a scale-free network (used in user study).*

4 Results and Discussion

4.1 Activity of Hubs

In scale-free networks, hubs have been shown to play an influential role on the dynamics. We first investigate this by looking into the excitation ratio of hubs. Figures 2(a) and (b) provide an interesting observation in the activity plot, namely that the nodes form a linear structure and we can sort the nodes of the network according to their position along a line. When brushing the activity plot to select the left-most nodes along the line, i.e., the nodes that are more often in a refractory state, we can observe from the highlighting in the linked degree map that the selected nodes correspond to nodes of high degree, i.e., hubs, see Figure 2(c) . This makes sense from an analytical point of view, as each node after excitation immediately goes into the refractory state. We, therefore, can reduce the dynamical space to the linear structure we detected. Approximating the linear structure with the horizontal order, we can define a descriptive dynamical parameter as the ratio $\frac{\#S}{\#S+\#R}$. It measures how often the state S occurs in the time series of a node to how often the states S or R occur.

Having identified this new descriptor, we can generate a 2D scatterplot that depicts the correlation of this 1D descriptor (dynamics) to the degree of the nodes (topology), see Figure 3. We can observe a clear dependence of the dynamics on the degree of the nodes.

Figure 2: *(a) Activity plot of dynamics on an excitable scale-free network which has adjacency matrix in Figure 1 with $n = 300$ nodes, $k = 2,500$ time steps, and parameters $f = 0.01$ and $p = 0.1$. (b) Brushing left-most nodes of linear structure in activity plot after zooming in. (c) Highlighting the brushed nodes in degree map exhibits that the selection represents the hubs.*

Figure 3: *2D scatterplot showing the correlation between the topological parameter of the degree of nodes and the detected dynamical parameter for activity.*

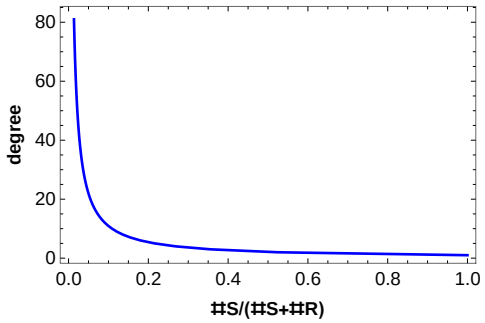

Figure 4: *Mean-field prediction for the numerical results from Figure 3 (p has same value, i.e., $p \approx 0.1$). The qualitative agreement about the relationship derived in Figure 3 is clearly visible.*

This dependence of the number of susceptible elements on the node degree can also be understood in a mean-field model of the discrete dynamical system, following [GM03, MLMH06, HL09, GLHH12]. Let $c_E(t)$, $c_S(t)$ and $c_R(t)$ be the density in the network at time t of excited, susceptible, and refractory nodes, respectively. The time course of these densities in a mean-field approximation is covered by the following discrete equations (in the limit of $f \to 0$; the general case is described in [HL09]):

$$\begin{aligned} c_E(t+1) &= c_S(t)c_E(t)k \\ c_R(t+1) &= c_E(t) + (1-p)c_R(t) \\ c_S(t+1) &= 1 - c_E(t) - c_R(t), \end{aligned} \tag{1}$$

which in the steady state ($c_X(t+1) = c_X(t)$) yield

$$c_S = 1/k,\ c_E = \frac{1-\frac{1}{k}}{1+\frac{1}{p}},\ c_R = \frac{c_E}{p} = \frac{1-\frac{1}{k}}{1+p}. \tag{2}$$

The quantity $\#S/(\#R+\#S) = c_S/(c_R+c_S)$ resulting from Eq. (2) is shown in Figure 4. The qualitative agreement between the relationship derived via our interactive data analysis and the mean-field result is clearly visible. Hence, we can conclude that using interactive visual means we could intuitively and reproduce the findings without using a priori knowledge about the processes.

4.2 Co-activation Waves Around Hubs

We want to examine whether we are able to re-produce the finding that hubs lead to propagation waves and want to test whether, in addition, our methods allow us to detect some interference patterns

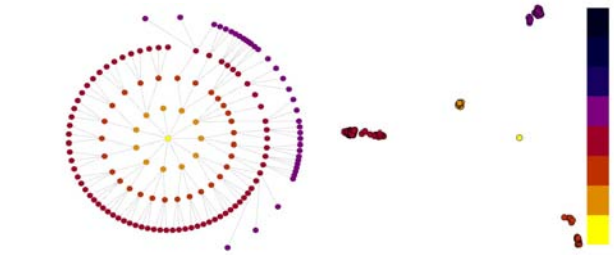

Figure 5: *(a) A network with tree topology (root is a hub) and (b) respective co-activation plot with $p = 0.1, f = 0.01$. The co-activation plot with color-coded topological distances to the hub exhibits the pattern that each cluster consists of nodes of equal distance to the hub.*

between hubs. We use the scale-free network, whose adjacency matrix is shown in Figure 1. We observe that no modular structure exists. Some hubs seem to exist, but their number and degree is not obvious. Using our degree map, we see that the network has four dominant hubs, see Figure 6(a).

We iteratively select the four dominant hubs one by one to examine the topological distances of the nodes to the hubs in the co-activation plot, see Figures 6(b)-(e). The co-activation plot exhibits four clusters. The two largest hubs are clearly responsible for form-

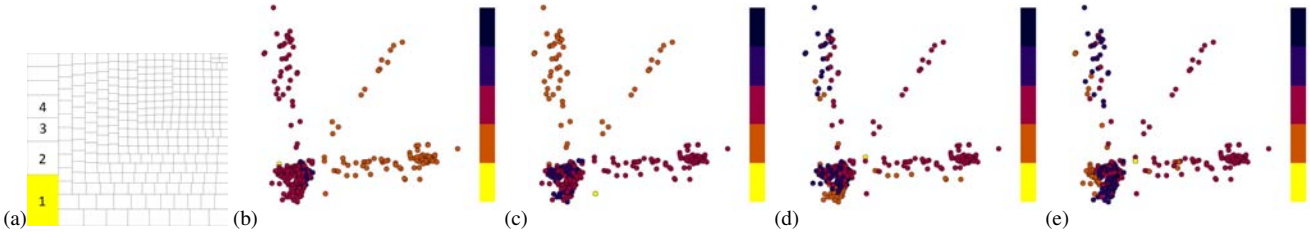

Figure 6: *(a) Selecting sequentially the four dominant hubs in degree map and (b-e) examining the co-activation plot ($p = 0.1, f = 0.01$) with color-coded topological distances to the selected hub reveals an interference pattern of propagation waves around the two largest hubs.*

ing these clusters, while the role of the third and fourth hub seems to be negligible. More precisely, the diagonal cluster in the upper right consists of exactly those nodes with distance 1 to both Hub 1 and Hub 2, the horizontal cluster in the lower right consists of exactly those nodes with distance 1 to Hub 1 and distance 2 to Hub 2, the vertical cluster in the upper left consists of exactly those nodes with distance 2 to Hub 1 and distance 1 to Hub 2, and the dense roundish cluster in the lower left consists of exactly those nodes with distance ≥ 2 to both Hub 1 and Hub 2. So, we can conclude that the largest two hubs are responsible for the dynamics in the scale-free network and, moreover, that there is an interference pattern of the propagation waves around those two hubs (the diagonal cluster in the upper right).

The structure of the dense roundish cluster in the lower left is not so obvious and seems to require further analysis. We interactively select this cluster in Figure 7(a) and re-compute the co-activation plot for only those points belonging to this cluster. Remarkably, the co-activation plot of that cluster exhibits again a very similar structure. We observe four sub-clusters with similar shapes as the clusters we had seen before. We use the coordinated views with the degree map to examine which topological structure is responsible for those four sub-clusters, see Figures 7(b) and (c). Interestingly, the sub-clusters are formed by the third and fourth hub. More precisely, one cluster has distance 1 to Hub 3, one cluster has distance 1 to Hub 4, one cluster has distance 1 to Hub 3 and Hub 4, and the last cluster has distance ≥ 2 to both Hub 3 and Hub 4. Hence, it is exactly the same interference pattern that we had observed for Hub 1 and Hub 2.

We can conclude that we could re-produce the finding that there are propagation waves emerging at hubs. Moreover, we were able to detect interference patterns between those waves and in contrast to Garcia et al. [GLHH12] we were able to do so without altering the topology. Finally, we were able to see that there is a combination of the degree of a hub and the distance to the hub that influences the dynamical pattern. This new finding will trigger future work in the field.

4.3 Synchonization Within Modules

Next, we want to re-produce the finding that modular structures lead to synchronization, which makes the functional structure coincide with the topological structure. We consider the hierarchical modular network, whose adjacency matrix is shown in Figure 8(a). The adjacency matrix exhibits three first-level modules. We can easily select them by brushing on the column next to the matrix and mark them using different colors. Figure 8(b) highlights to selected modules in the co-activation plot using matching colors. We can observe that there is a one-to-one match between the modules and the co-activation clusters.

We continue the analysis by selecting one of the co-activation clusters and re-compute the co-activation plot for that cluster only, see Figures 8(b) and (d). We go back to the adjaceny matrix and select the five second-level modules of the selected first-level module, see Figures 8(c). Highlighting the second-level modules in the refined co-activation plot reveals that the second-level modules also match sub-clusters of the selected cluster, but that the match is not perfect anymore.

We can conclude that the synchronization within modules can be confirmed, but we also noticed that the synchonization strength decreases with the hierarchical level. This can be explained by the fact that the second-level modules are less separated than first-level modules.

4.4 Interplay of Hubs and Modules in Connectome

Finally, we look into the empirical networks representing the connectomes as described in Section 2.1.3. Such networks contain both modular structures and hubs. Figure 9(a) shows the adjacency matrix for cat. We can select two modules and observe their pattern in the co-activation plot, see Figure 9(b). Indeed, they form two clusters, but the clusters are not clearly separated, as they seem to merge at the top.

We investigate the role of hubs by switching to the degree map. Since this is a directed network, we consider the out-degree, as nodes with large out-degree influence their neighbors most. The node which has the maximum out-degree is selected, see Figure 10(a). We can observe from the co-activation plot (Figure 10(b)) that the hub is located in the area where the clusters in Figure 9(b) come together. The same is true for the second- and third-largest hubs. Hence, the hubs serve as bridges between the modules. The macaque network revealed the same structure and we made the same observations (cf. accompanying video).

4.5 Expert Evaluation

We evaluated our approach in a qualitative user study with five domain experts working in computational systems biology including

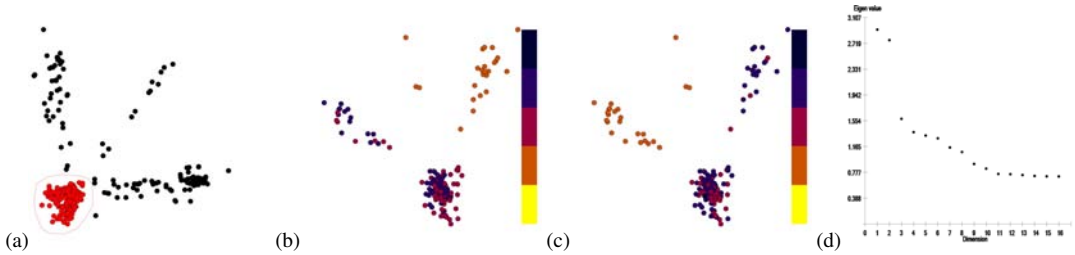

Figure 7: *(a) Selecting a cluster in the co-activition plot and (b,c) re-computing the co-activation plot for the selection reveals sub-clusters with interference pattern for Hubs* 3 *and* 4 *similar to that of original clusters. (d) Eigenvalue plot for MDS projection used to compute the co-activation plot for selected cluster.*

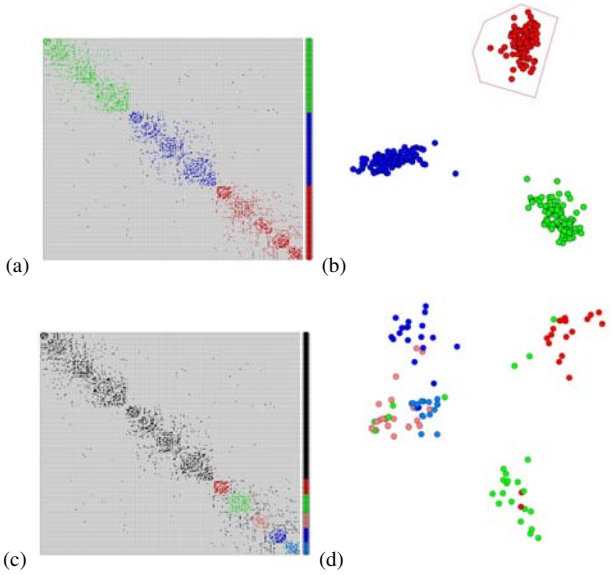

Figure 8: *(a) Selecting first-level modules in the adjacency matrix (b) reveals matching clusters in the co-activation plot ($p = 0.1, f = 0.01$). Selecting one clusters and (d) re-computing the co-activation plot for that clusters reveals less obvious sub-clusters (c) that somewhat match second-level modules.*

four post-doctoral fellows with 5 to 23 years of experience in the field and one fourth-year PhD student. We first gave them an introduction to the approach and made them familiarize themselves with the interactions. Then, they were asked to perform analyses with our tool using different topologies (with a focus on scale-free networks). Their task was to check how modules and hubs influence the co-activation patterns (propagation waves, interference, synchonization) for different parameter settings. Afterwards, they were asked to answer to a questionnaire, where we asked them to rate our tool's usefulness (to what degree our tool helps to solve their analysis tasks), intuitiveness (how easily they can interpret the visual encodings and handle the interactions), and potential to support traditional analysis on a 5-step Likert scale. We also asked for further comments concerning what they liked in particular and where they saw limitations and space for extensions.

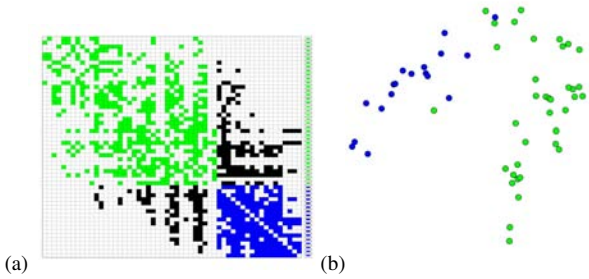

Figure 9: *Co-activation patters of two modules in the cat cortical network for $p = 0.1, f = 0.005$. In the co-activation plot, the two clusters are not clearly separated, as they seem to merge at the top.*

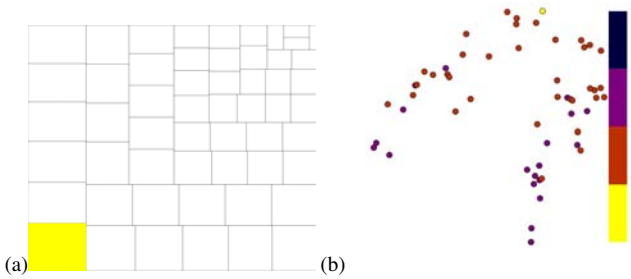

Figure 10: *Co-activation patterns of the biggest hub (out-degree) in the cat cortical network. The merging part at the top in the co-activation plot includes nodes having distance* 1 *to the selected hub.*

All five domain experts rated that our tool is useful (rating 4). Concerning the intuitiveness, four of the users rated our tool to be intuitive (rating 4) and one even considered it very intuitive (rating 5). With respect to the ability to support traditional analysis, again all post-doctoral fellows rated our tool as being helpful (rating 4), while the PhD student felt he was not senior enough to judge this. They pointed out that they particularly appreciated the easiness to explore excitation dynamics on new data sets. For instance, when performing the analysis with different parameter configurations, they see the range of parameter values, where topology can explain dynamical patterns, and the range of parameter values, where dynamics no longer follow the topology. The degree map was a new

concept to them, but they immediately felt comfortable in using it to identify hubs. Also color-coding the distance to hubs was an intuitive feature for them.

In terms of limitations, they wanted to not only switch between degree map and adjacency matrix, but also wanted to have them side-by-side using coordination to see whether hubs belong to modules, which we will incorporate in our next version. In terms of extensions, they asked for more information about the nodes (name, connectivity, etc.) that they identified as outliers in the co-activation plot. Hence, our tool is intuitive and triggers further analyses. However, one of them raised doubts about the ability of the adjacency matrix layout to detect hierarchical structures in the network. According to their experience, they hypothetically expected other topological structures such as fractal or some different small motifs like feed-forward loop, etc., shape the co-activation pattern as well, and our approach does not support answering such hypotheses yet.

4.6 Further Discussion

Comparison to time series visualization. Dynamical data is typically analyzed using time series plots. However, the goal of this approach is the analysis of how topology governs dynamics under the effect of noise (using f and p), where time series plots (as well as animations) are of very limited use. Looking at all the time series plotted over time would reveal a somewhat random pattern and it would be hard (if not impossible) to analyze systematically the influence of topology on the dynamics. Therefore, deriving properties such as co-activation or excitation ratio is more useful.

Order in adjacency matrix. A proper order of the nodes in the adjacency matrix is of utmost importance. We use the barycenter ordering, because it generally produces good results and is simple to implement. However, the ordering is based on a heuristic algorithm, so for some cases some nodes within a module are ordered differently as nodes within other modules. Therefore, the ordering is not always perfect. However, misplaced nodes in the adjacency matrix are typically quickly identified using our interactive system by having individual nodes of a module not appearing in the cluster. Hence, our interactive system allows for the detection and handling of such cases.

Scalability. Using the adjacency matrix layout has the advantage of scaling better to larger networks than, e.g., node-link diagrams. Also, the degree map scales quite well, as it is used to investigate hubs, which are represented by large rectangles even if many small rectangles may not be visually distinguishable anymore. In fact, it would be fine to eliminate nodes with very small degree from the degree map. The co-activation plot and activity plot show the nodes as points, which is the least visually complex geometry, i.e., scalability is good and points overlapping to form clusters are actually desirable.

The influence of parameters. Our system allows for quickly exchanging parameter settings and thus explore the parameter space. For example, changing f and p in the activity plot in Figure 2(a) leads to a movement of the linear structure towards the barycenter when increasing f and towards the lower left when increasing p. Moreover, we applied our approach for different parameters configurations, e.g., we fix $p = 0.1$, and run tests for f from 0.01 to 0.15 for the macaque cortical network (cf. accompanying video). We observe that, from $f = 0.15$ on, the co-activation pattern presents no synchronization patterns of modules anymore. Observing how much topology constraints dynamics for different noise configurations relates our application to explaining the transition phases of complex system. For small amount of noise the dynamics follow topology (order phase), but for large amount of noise this is not true anymore (chaotic phase).

5 Conclusion

We have presented a visual analysis approach for tackling one of the most challenging classic problems in biological computing, namely to understand how topology shapes dynamics in excitable networks. Our approach allows for a quick and intuitive analysis. Hence, we were able to quickly confirm findings made in the literature in a systematic way. Moreover, we were also able to detect new findings, which will trigger future work in the application field. The design lesson learnt was that different properties of the data required us to use different visual encodings of given data attributes as well as derived data attributes. Linking these different encodings with coordinated views allowed us to gain insight into their interplay. This concept cannot only be generalized to other excitable (such as the Kuramoto [TPHL12] or the Fitzhugh-Nagumo model [MHKH15]) or non-excitable network dynamics, but it generalizes to any time series data over any graph structure.

Acknowledgments. This work was supported by the Project on International Education Development for Universities and Colleges of Vietnam (project no. 911).

References

[AKK*10] ALBRECHT M., KERREN A., KLEIN K., KOHLBACHER O., MUTZEL P., PAUL W., SCHREIBER F., WYBROW M.: On open problems in biological network visualization. In *Graph Drawing* (2010), Springer, pp. 256–267. 3

[BB03] BARABÁSI A.-L., BONABEAU E.: Scale-free networks. *Sci. Am. 288*, 5 (2003), 50–59. 2

[BBDW14] BECK F., BURCH M., DIEHL S., WEISKOPF D.: The state of the art in visualizing dynamic graphs. *EuroVis STAR* (2014). 2

[BHVW00] BRULS M., HUIZING K., VAN WIJK J. J.: *Squarified treemaps*. Springer, 2000. 4

[BLM*06] BOCCALETTI S., LATORA V., MORENO Y., CHAVEZ M., HWANG D.-U.: Complex networks: Structure and dynamics. *Phys. Rep. 424*, 4-5 (Fervier 2006), 175–308. 2

[BPF14] BACH B., PIETRIGA E., FEKETE J.-D.: Visualizing dynamic networks with matrix cubes. In *Proceedings of the SIGCHI Conference on Human Factors in Computing Systems* (2014), ACM, pp. 877–886. 2

[Bra01] BRANKE J.: Dynamic graph drawing. In *Drawing Graphs*, Kaufmann M., Wagner D., (Eds.), vol. 2025 of *Lecture Notes in Computer Science*. Springer Berlin / Heidelberg, 2001, pp. 228–246. 2

[CC00] COX T. F., COX M.: *Multidimensional Scaling, Second Edition*, 2 ed. Chapman and Hall/CRC, 2000. 5

[EDG*08] ELMQVIST N., DO T.-N., GOODELL H., HENRY N., FEKETE J.-D.: Zame: Interactive large-scale graph visualization. In *Visualization Symposium, 2008. PacificVIS'08. IEEE Pacific* (2008), IEEE, pp. 215–222. 2

[EMB*09] EL BOUSTANI S., MARRE O., BÉHURET S., BAUDOT P., YGER P., BAL T., ET AL.: Network-state modulation of power-law

frequency-scaling in visual cortical neurons. *PLoS Comput Biol 5*, 9 (2009). 2

[Fek09] FEKETE J.-D.: Visualizing networks using adjacency matrices: Progresses and challenges. In *Computer-Aided Design and Computer Graphics, 2009. CAD/Graphics '09. 11th IEEE International Conference on* (aug. 2009), pp. 636 –638. 2, 4

[FW10] FORLINES C., WITTENBURG K.: Wakame: sense making of multi-dimensional spatial-temporal data. In *Proceedings of the International Conference on Advanced Visual Interfaces* (2010), ACM, pp. 33–40. 3

[GAA04] GATALSKY P., ANDRIENKO N., ANDRIENKO G.: Interactive analysis of event data using space-time cube. In *Information Visualisation, 2004. IV 2004. Proceedings. Eighth International Conference on* (2004), IEEE, pp. 145–152. 3

[GFV13] GIBSON H., FAITH J., VICKERS P.: A survey of two-dimensional graph layout techniques for information visualisation. *Information visualization 12*, 3-4 (2013), 324–357. 2

[GLHH12] GARCIA G. C., LESNE A., HÜTT M.-T., HILGETAG C. C.: Building blocks of self-sustained activity in a simple deterministic model of excitable neural networks. *Frontiers in computational neuroscience 6* (2012). 1, 2, 3, 6, 7

[GM03] GRAHAM I., MATTHAI C. C.: Investigation of the forest-fire model on a small-world network. *Physical Review E 68* (2003), 036109. 6

[HBO*00] HILGETAG C.-C., BURNS G. A., O'NEILL M. A., SCANNELL J. W., YOUNG M. P.: Anatomical connectivity defines the organization of clusters of cortical areas in the macaque and the cat. *Philosophical Transactions of the Royal Society of London B: Biological Sciences 355*, 1393 (2000), 91–110. 2

[HH14] HILGETAG C. C., HÜTT M.-T.: Hierarchical modular brain connectivity is a stretch for criticality. *Trends in cognitive sciences 18*, 3 (2014), 114–115. 1

[HK04] HILGETAG C. C., KAISER M.: Clustered organization of cortical connectivity. *Neuroinformatics 2*, 3 (2004), 353–360. 2

[HKH14] HÜTT M.-T., KAISER M., HILGETAG C. C.: Perspective: network-guided pattern formation of neural dynamics. *Philosophical Transactions of the Royal Society B: Biological Sciences 369*, 1653 (2014), 20130522. 2, 3

[HL09] HÜTT M., LESNE A.: Interplay between topology and dynamics in excitation patterns on hierarchical graphs. *Front. Neuroinform. 3* (2009). 2, 6

[HMM00] HERMAN I., MELANÇON G., MARSHALL M. S.: Graph visualization and navigation in information visualization: A survey. *IEEE Transactions on Visualization and Computer Graphics 6* (January 2000), 24–43. 2

[HSCW13] HADLAK S., SCHUMANN H., CAP C. H., WOLLENBERG T.: Supporting the visual analysis of dynamic networks by clustering associated temporal attributes. *Visualization and Computer Graphics, IEEE Transactions on 19*, 12 (2013), 2267–2276. 4

[JKS06] JUNKER B. H., KLUKAS C., SCHREIBER F.: VANTED: a system for advanced data analysis and visualization in the context of biological networks. *BMC Bioinformatics 7* (2006), 109. 3, 4

[LPP*06] LEE B., PLAISANT C., PARR C. S., FEKETE J.-D., HENRY N.: Task taxonomy for graph visualization. In *Proceedings of the 2006 AVI Workshop on BEyond Time and Errors: Novel Evaluation Methods for Information Visualization* (2006), BELIV '06, pp. 1–5. 2

[McG12] MCGUFFIN M. J.: Simple algorithms for network visualization: A tutorial. *Tsinghua Science and Technology 17*, 4 (2012), 383–398. 4

[MFL*16] MA C., FORBES A. G., LLANO D. A., BERGER-WOLF T., KENYON R. V.: Swordplots: Exploring neuron behavior within dynamic communities of brain networks. *Journal of Imaging Science and Technology 60*, 1 (2016), 10405–1–10405–13(13). 3

[MHKH15] MESSE A., HÜTT M.-T., KONIG P., HILGETAG C. C.: A closer look at the apparent correlation of structural and functional connectivity in excitable neural networks. *Sci. Rep. 5*, 7870 (2015). 1, 2, 3, 9

[MKF*15] MA C., KENYON R. V., FORBES A. G., BERGER-WOLF T., SLATER B. J., LLANO D. A.: Visualizing dynamic brain networks using an animated dual-representation. In *Proceedings of the Eurographics Conference on Visualization (EuroVis)* (2015), pp. 73–77. 3

[MLB10] MEUNIER D., LAMBIOTTE R., BULLMORE E. T.: Modular and hierarchically modular organization of brain networks. *Frontiers in neuroscience 4* (2010). 2

[MLHH08] MÜLLER-LINOW M., HILGETAG C. C., HÜTT M.-T. .: Organization of excitable dynamics in hierarchical biological networks. *PLoS Comput Biol 4(9)* (2008). 1, 2, 3

[MLMH06] MÜLLER-LINOW M., MARR C., HÜTT M.: Topology regulates the distribution pattern of excitations in excitable dynamics on graphs. *Physical Review E 74*, 1 (July 2006), 1–7. 2, 6

[MM13] MORETTI P., MUÑOZ M. A.: Griffiths phases and the stretching of criticality in brain networks. *Nature communications 4* (2013). 1

[NM10] NAKAO H., MIKHAILOV A. S.: Turing patterns in network-organized activator-inhibitor systems. *Nature Physics 6*, 7 (2010), 544–550. 1

[PS08] PAN R. K., SINHA S.: Modular networks with hierarchical organization: The dynamical implications of complex structure. *Pramana 71*, 2 (2008), 331–340. 2

[RS10] RUBINOV M., SPORNS O.: Complex network measures of brain connectivity: uses and interpretations. *Neuroimage 52*, 3 (2010), 1059–1069. 2

[SBM*14] STEIGER M., BERNARD J., MITTELSTÄDT S., LÜCKE-TIEKE H., KEIM D., MAY T., KOHLHAMMER J.: Visual analysis of time-series similarities for anomaly detection in sensor networks. *Computer Graphics Forum 33*, 3 (2014), 401–410. 4

[SCKH04] SPORNS O., CHIALVO D. R., KAISER M., HILGETAG C. C.: Organization, development and function of complex brain networks. *Trends in cognitive sciences 8*, 9 (2004), 418–425. 2

[Spo13] SPORNS O.: Structure and function of complex brain networks. *Dialogues in clinical neuroscience 15*, 3 (2013), 247. 1

[SSK14] SAKET B., SIMONETTO P., KOBOUROV S.: Group-Level Graph Visualization Taxonomy. In *EuroVis - Short Papers* (2014), Elmqvist N., Hlawitschka M., Kennedy J., (Eds.), The Eurographics Association. 2

[Tam13] TAMASSIA R.: *Handbook of graph drawing and visualization*. CRC press, 2013. 2

[Tol96] TOLLIS I. G.: Graph drawing and information visualization. *ACM Comput. Surv. 28*, 4es (Dec. 1996). 2

[TPHL12] TOOSI F. G., PAULOVICH F. V., HÜTT M.-T., LINSEN L.: Projection-based visualization of dynamical processes on networks. *EuroVis-Short Papers* (2012), 61–65. 4, 9

[vLKS*11] VON LANDESBERGER T., KUIJPER A., SCHRECK T., KOHLHAMMER J., VAN WIJK J., FEKETE J.-D., FELLNER D.: Visual analysis of large graphs: State-of-the-art and future research challenges. *Computer Graphics Forum 30*, 6 (2011), 1719–1749. 2

[War12] WARE C.: *Information Visualization, Perception for Design (Interactive Technologies)*, 3 ed. Morgan Kaufmann, 2012. 5

[You93] YOUNG M. P.: The organization of neural systems in the primate cerebral cortex. *Proceedings of the Royal Society of London B: Biological Sciences 252*, 1333 (1993), 13–18. 2